Development and Testing of an Ultraviolet Light Monitor for Fluorescence Microscopy

Javier Eduardo Diaz-Zamboni
and Víctor Hugo Casco

Current quantitative analysis in fluorescence microscopy considers that in the image formation process of the microscope, the sample behaves as a fluorescent stable-emitter. However, it is very well known that the flux from ultraviolet lamps is variable throughout their useful life and as time passes, such variations are incremented in rate and amplitude. For this reason, it is crucial to consider systematically these variations in images when quantitative methods are required in modern microscopy. In this article, we show the development of a very simple device and method to test and measure these variations. We also propose software to correct such fluctuations in quantitative microscopy studies.

Introduction

Quantitative microscopical analysis has historically been an important technique in molecular and cell biology (Arndt-Jovin *et al.*, 1985). This allows signalling from specific structures within the specimen. The usual method to establish positive reactions is by using contrast to compare signal versus control images, or different levels of signal that could eventually come from different biological alteration models. Because of this, it may require comparison of multiple images, which in some cases may have been obtained using different microscopes.

These powerful techniques are affected by several variables, which, in general terms, can be classified as those concerned with specimen preparation and those linked to image registration or processing. This work is focused on lamp instability associated with the second type of variable, which is a major source of noise in fluorescence microscopy and hard to control. Therefore, it should be taken into account when quantitative methods are required in image processing and analysis (Swedlow, 2007).

As is well known, mercury and xenon arc lamps produce light that ranges from ultraviolet to infra-red (henceforth referred to as UV-lamp and UV-light respectively). In classical fluorescence microscopy, they are the excitation source of fluorophores providing the necessary wavelengths to stimulate molecular fluorescence. They are supposed to be stable in their illumination flux; however, in practice this is not true, since even in optimum control conditions of the power source, lamps flicker throughout their useful life. This phenomenon is the result of instabilities in the gas plasma, which is highly affected both by magnetic fields and the erosion of the electrodes. There is a short-term instability that represents 2 - 10% of the total flux intensity and it is in the order of milliseconds to seconds. In mercury gas lamps, as time passes, this flicker effect increases in rate and amplitude and the intensity weakens with prolonged use, since metal vapours from electrodes become deposited on the glass envelope (Chen *et al.*, 1995; Chen, 1995a; Murphy, 2001).

This variability in the illumination flux of the scene has a strong effect on imaging. For example, in a charged coupled device (CCD), the resulting intensities of the images captured are directly related to the electrical charges stored in the CCD because light is detected through a cumulative process. Photons from the scene are stored as electrical charges in each element of the array during the exposure (Hiraoka *et al.*, 1987; Young, 1996). Hence, any variation of the incident light source will affect the image.

This temporal variability of the illumination is even more critical in multidimensional imaging, as in optical sectioning or time lapse studies, where the problem can be observed in consecutive images (Figure 1). Lamp instabilities introduce high frequency variations, which are not genuine distortions of the optical system and that are not considered in the usual algorithms of analysis and quantification, such as deconvolution or ratio image analysis (Sibarita, 2005). Thus, any post processing or analysis would produce artefactual images or erroneous results respectively.

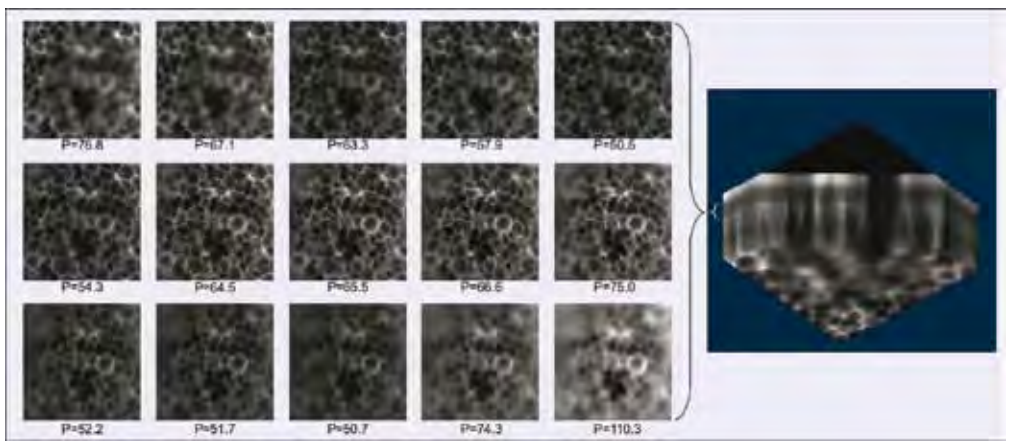


Fig. 1. Fifteen optical sections of FITC-tagged adhesion molecules in skin of Rhinella arenarum, captured with a 20 x objective lens, NA=0.4. Displacement in Z, 1 µm. Left: gallery view. P values represent mean intensity on each image. Right: Stack projection of the sections with para-axial cut showing light fluctuations in optical sections.

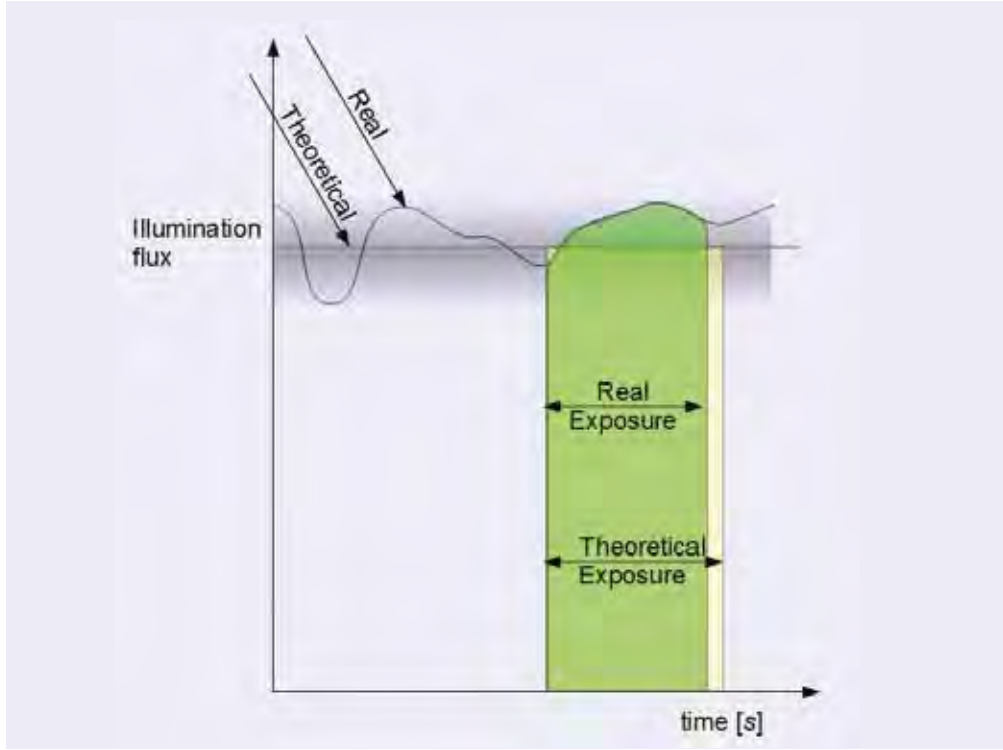


Fig. 2. The system developed compensates for the exposure, integrating numerically the samples obtained by the UV-light monitor, thus fitting the dosage to the expected value (theoretical illumination flux).

It is possible to reduce the flicker effect on images with multiple image captures and then obtaining the images' average appearance. However, this technique introduces some restrictions that make it unsuitable in some cases because it reduces sampling rates and prolongs light exposure resulting in photo-bleaching and photo-damage (Song *et al.*, 1999).

To solve this problem, we have developed an easy-to-make and rapid-to-mount UV-light monitor for an epifluorescence microscope that allows us for the first time to have a precise measurement of the light levels supplied by the UV-lamp. Basically, the hardware is based on a light sensor and a voltage-frequency converter, which is connected to the microscope's computer. The control software was built based on an application program interface (API) that controls the data acquisition of the UV-light monitor. This module was embedded in our microscope control software, SUMDD (Diaz-Zamboni, 2004). Based on this configuration, it is possible to register an image with a pre-set exposure time and the dose is then measured automatically and stored with the image. Alternatively we can capture an image, controlling the exposure time until a pre-determined light dosage is achieved, as is schematically shown in Figure 2.

A systematic evaluation of the system has been undertaken. The tests can be divided into two groups. First of all, we carried out the measurements and analysis on the circuit in order to establish the operating conditions of the circuit and sensor. After that, evaluations were conducted on the entire system, to have a comprehensive appraisal of the development.

Materials and methods

Hardware

The microscope system was based on an Olympus BX50 upright fluorescence microscope. The excitation source for fluorescence was a mercury-arc lamp, which can be filtered by three different Olympus cube filters: U-MWU (Exc.: BP330-385, Dic. Mirror: DM400 and Em.: BA420), U-MWIB (Exc.: BP460-490, Dic. Mirror: DM505 and Em.: BA515IF) and U-MSWG (Exc.: BP480-550, Dic. Mirror: DM570 and Em.:BA590). The recording system consisted of an Apogee CCD camera (Model AM4), with a sensor of 768 x 512 square pixels, with sides 9 µm long, 14 bits of resolution, a Peltier cooling system and attached to the microscope via a 0.5 C-mount lens. In addition, a stepping motor RS 440-436 was connected to the micro-metric screw of the microscope, through a 100:1 reducing box (Adur & Schlegel, 1997).

The UV-light monitor was based on a very simple electronic circuit. We used a common green light emitting diode (LED) as a light sensor, which has been shown to produce a current in the presence of light (Ferrero, 1999). Light generates photo-electrons on the PN-junction of the LED, which is in parallel with a resistance, producing a proportional voltage drop across it. The potential difference is amplified by a TL081 operational amplifier configured as a non-inverter adder (National Semiconductor Corporation, 1995). The output of the op-amp is converted to frequency by a LM555 timer in a bi-stable configuration (National Semiconductor Corporation, 2006) whose output is wired and plugged to the microphone input of the microscope's computer.

Software

We have also developed software named SUMDD (Diaz-Zamboni, 2004) which controls both the camera via an ISA card and the stepping motor via a parallel port, allowing image capture, focusing by keyboard, optical sectioning and 3D deconvolution and visualisation.

An API was developed in Object Pascal language to acquire the data through the sound card. This API was associated with the microscope control software and by means of a main frequency detection algorithm, the light level was captured. Basically, the frequency detection algorithm first reduces the amplitude of harmonics with a low-pass filter and then a transformation of the resulting data to the Fourier frequency space determines the position of the maximum in the power spectrum to estimate the fundamental frequency. This frequency value is transformed via a calibration curve to calculate a light level. For dose determination, the samples of the UV-light monitor are integrated numerically immediately after a new sampled value reaches the processing buffer.

Methodology

The system's operating environment was determined. In particular the effect of temperature on the detector's sensitivity was studied, since it was located within the lamp housing and, therefore, would be subject to high temperatures due to its proximity with the light source. The temperature was monitored with a thermocouple to establish the temperature working range. In parallel, we analysed and established the optimal parameters of the UV-light monitor in order to obtain optimum performance in relation to the control hardware's constitutive blocks: sensor conditioning stage, voltage-frequency block and digitisation.

Although the linearity of the sensor response is guaranteed (Ferrero, 1999), there were intermediate steps in the development that modified the captured signal and these had to be taken into account. The second block is a voltage-frequency converter that has an exponential response and it needed to be linearised to correctly determine the dose. For this, a test was conducted which consisted of determining the response of the voltage-frequency converter circuit for different input values. The measurements were carried out in two ways: a frequency meter with a fundamental frequency detection algorithm, developed for this purpose. With both sets of measurements, the correlation coefficient was calculated to establish the similarity between the sets of measurements.

According to Ferrero (1999), the proposed detector has a spectral response guaranteed within the visible spectrum. Because of this, an analysis of its response within the range of excitation of the interference filters was done. To do this, a detector was focused with a 40 x objective lens and its response was evaluated on the incident intensity for each excitation filter of the microscope.

For the integrated evaluation of the system, we analysed two important parameters: the linearity in the image-dose determination, that is to say, the accumulated light during a given exposure time and the ability to compensate the exposure against the changes of the incident light.

The camera technology used allows control of the whole camera through an API, making use of a set of functions and state variables. While the programming was simplistic, with this configuration it was necessary to evaluate and validate the linear response in dose determination making use of a precise timer. This was because the dose was calculated in parallel with exposure and there was no control for all the other involved variables (i.e. numerical conversions, CCD image interval read out, etc.). Thus, we programmed an experiment, which consisted of the determination of the dose by means of two types of acquisition. One was a simulated image exposition, with a computer timer. The experiment was repeated ten times, each one consisting of 100 samples with exposure times randomly selected between 0.1 seconds and 5.0 seconds. We measured the proportionality between dose and exposure time, as well as measuring the correlation between the simulated and real captures. Linear regressions were performed on the results and finally compared with a t-test to determine significant differences between the methods.

To evaluate if the system would properly correct the shortcomings of the illumination flux, a set of tests was performed in order to determine if the corrected exposure time was able to compensate the intensity levels in images. Thus, several time series analyses of homogeneous fluorescent solutions and sub-resolution fluorescent micro-beads were made, where the measurement parameter used to establish the correct exposure time compensation was the right fit to the mono-exponential and bi-exponential photo-bleaching curves (Ghauharali *et al.*, 1998). Three groups of measurements were compared: normal image capture, image capture averages (usually used for correcting illumination defects) and finally capturing the series of images with dose compensation. Three samples were prepared from homogeneous solutions of FITC (Sigma Chemical Company, St. Louis, USA). From each sample, three series of images were obtained: (1) normal capture, (2) averaging and (3) controlled exposure. Similarly, three solutions of fluorescent micro-beads from the F-8888 kit (Molecular Probes, Eugene, OR, USA) were processed in the same way. For all cases, an exposure time of 1 second, 3 seconds inter-image interval and 30 frames per series were used.

The proposed image analysis was developed as a plug-in for ImageJ (Rasband, 1997–2010). It analyses an image-time series where it is possible to set two parameters for analysis: number of samples (as regions of interest, ROIs) on the series and size of the ROIs. The program generates ROIs of the pre-set size and randomly locates them. For each ROI, it calculates the average intensity on each image of the series. Then the photo-bleaching mono-exponential and bi-exponential curves are fitted against time (Flanagan, 2010).

Results

Test and results on electronic circuit preparation can be seen in the section Additional Information, which can be found at www.infocus.org.uk.

The image capture simulation tests showed that the UV-light monitor is independent of image capture and responds linearly to increments in exposure times. Figure 3 shows the linear regressions of the dose measurements making a real capture and a simulated capture.

Table 1 gives the results of the 10 simulations. In all of the simulations, the regressions have shown independence in the dose determination and a linear stable behaviour as the exposure time increases. From Figure 3 and Table 1, it is observed that the magnitude of the slope is similar in both regressions; thus, we performed an independent t-test, to establish whether in the 10 experiments there were significant differences between dose measurements with a precise timer and using the state variables of the CCD device.

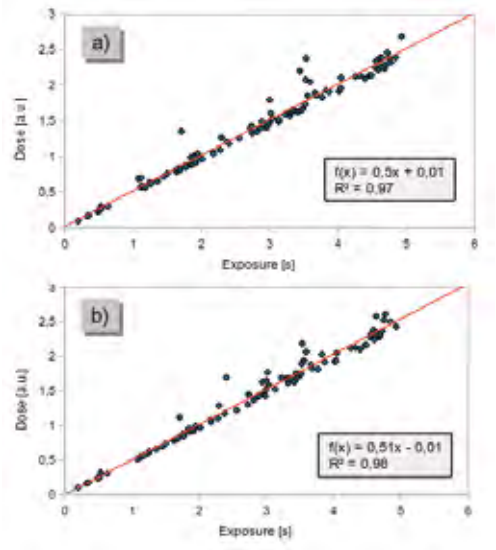


Fig. 3. Scatter plot and linear regressions of the dose measurement made when a) real and b) simulated images are captured.

Experiment	Regression data for real captures		Regression data for simulated captures	
	Slope	R2	Slope	R2
1	0.50	0.99	0.52	0.96
2	0.49	0.99	0.49	0.98
3	0.49	0.96	0.49	0.97
4	0.50	0.98	0.49	0.98
5	0.51	0.95	0.49	0.98
6	0.49	1.00	0.49	1.00
7	0.50	1.00	0.49	1.00
8	0.49	0.95	0.50	0.97
9	0.51	0.94	0.51	0.94
10	0.50	0.97	0.51	0.98

Table 1: Tests made on simulated and real image captures. An independent t-test was also performed on the slope data and that showed that there were not significant differences between their means with 99% confidence.

Cube filters light level [v]			Cube filter light level ratios		
U-MWIB (BP460-490)	U-MSWG (BP480-550)	U-MWU (BP330-385)	U-MWIB/ U-MSWG	U-MWU/ U-MSWG	U-MWU/ U-MWIB
0.30	1.26	0.06	0.24	0.05	0.22
0.25	1.14	0.06	0.22	0.05	0.25
0.22	1.03	0.05	0.21	0.05	0.24
0.21	0.94	0.05	0.22	0.05	0.24
0.19	0.84	0.04	0.23	0.05	0.23
0.15	0.65	0.03	0.23	0.05	0.23
0.11	0.51	0.03	0.22	0.05	0.25
Mean			0.22	0.05	0.23
Standard Deviation			0.01	0.00	0.01

Table 2: Light level captured with three filters mentioned previously. Ratios between filters were calculated and they showed no changes for different light levels.

The sensor response to the three different excitation wavelength ranges was analysed focusing a detector with the 40 x objective lens. At the same time, the detector in the lamp housing was detecting light levels from the lamp.

The light level was measured for each filter and the ratio of intensities between filters was calculated, as the aperture diaphragm was gradually closed from its maximum. Results are shown in Table 2.

The average light level in the lamp housing was 0.50, while the between filter ratios showed a stable behaviour against light level variations.

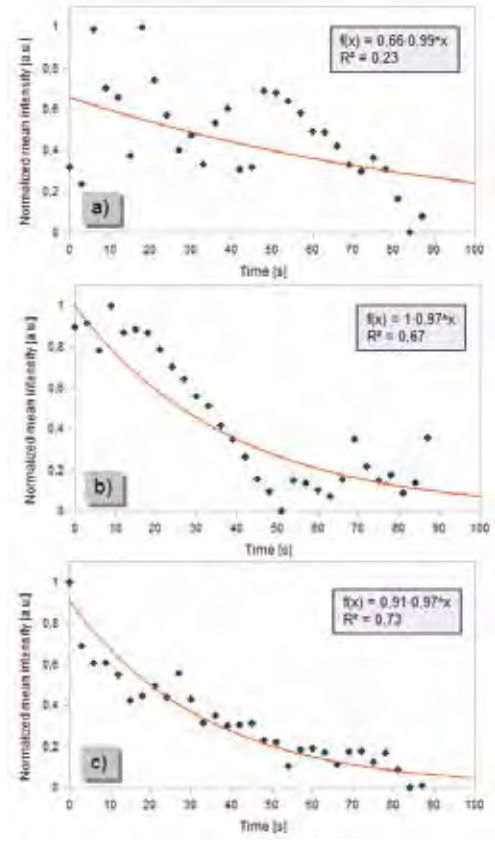


Fig. 4. Mono-Exp fitting curves of photobleaching of homogeneous solutions of FITC. Time series were captured once the lamp had reached a stable state. Each value was obtained as an average of a ROI for each image: a) normal exposure, b) capture average and c) controlled capture.

Image analysis

Figures 4 and 5 show examples, from the set of the captured time series of the FITC solutions, of two possible situations in fluorescence microscopy. In the former, it is easy to note the poor photo-bleaching curve fitting, where the lamp had a high level of flickering. This case was specially selected just after the lamp began to emit light, showing high variations due to the unstable gas plasma. On the other hand, Figure 5 shows a better photo-bleaching curve fitting: this is a time series made 30 minutes after the lamp was turned on. The results of the photo-bleaching curve fitting were normalised in order to make them comparable. Moreover, this normalisation allowed us to distinguish the differences in intensities, which are not easily visible in the dynamic range of the CCD.

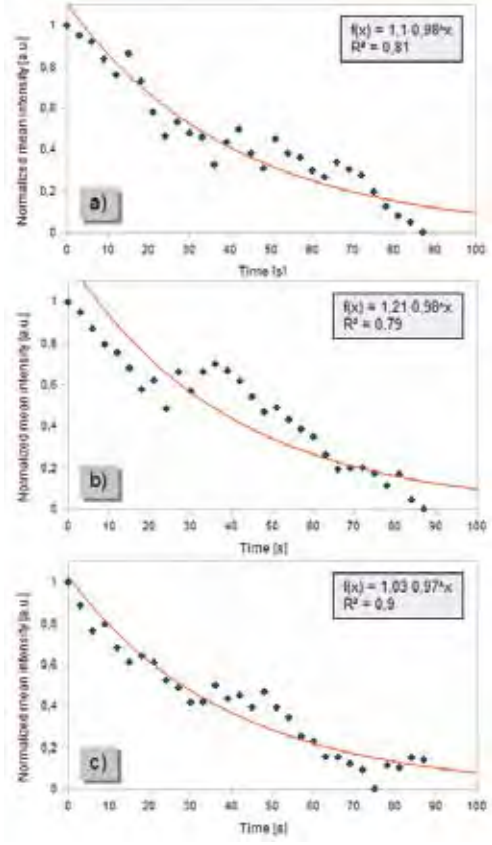


Fig. 5. Mono-Exp fitting curves of photobleaching of homogeneous solutions of FITC. Time series were captured when the lamp had not reached a stable illumination flux. Each value was obtained as an average of a ROI for each image: a) normal exposure, b) capture average and c) controlled capture.

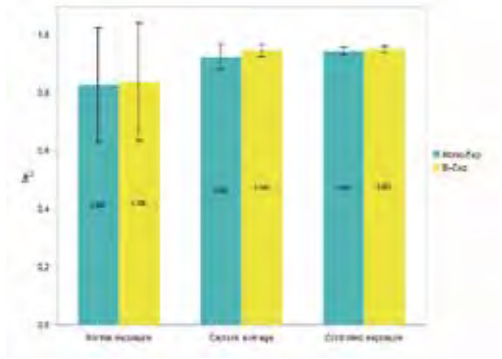


Fig. 6. Bar graph showing the photobleaching regression curves made on time series images of the homogeneous solutions of FITC captured using the three different techniques. Coloured bars are the mean of the R2 calculated for each curve regression. Black bars, at the top, show standard deviations. For all cases analysed, the use of the UV-light monitor showed the best fitting curves and the lowest scatter.

Figure 6 shows results of the photo-bleaching regressions curves made from FITC solutions. There is a noticeably good performance of the regression algorithms applied to the FITC solution images. See results of the analysis of micro-bead images in the Additional Information section.

Conclusion and Discussion

We have developed an easy-to-make UV-light monitor that allows us to have a new parameter to analyse images taken with a fluorescence microscope. The device provides exposure time compensation by dose calculation.

In the vast majority of applications of quantitative fluorescence microscopy, it is a requirement to compare multiple images, which in some cases may have been taken with different microscopes. Due to the inherent differences of different microscope systems, a method has been proposed for image standardisation based on the photobleaching curve of a test layer (Ghauharali & Brakenhoff, 2000). This work uses these conceptual ideas for evaluating this development. It complements this image standardisation method because using the direct method reported here for correcting the temporal fluctuations of the light and the generated curve fit will be much more accurate. It also introduces a new parameter for comparing images and light dosage.

The dose is determined using arbitrary units. To give it in absolute units, it is necessary to make a calibration using a radiometer. Calibration will give us a useful device for comparing images between different systems, such as laser confocal microscopy, where illumination dosage may be finely controlled. Despite the extra work involved, the system reported here is useful for the analysis of images of a same microscope, whose illumination parameters are time-varying. After completing calibration, we will be able to include with the microscope control software the functionality of image capturing using dosage levels instead of exposure time of the CCD.

With the dose determination, it is possible to establish how much energy is required to damage a specimen by photo-bleaching or photo-damage or it may be necessary for light dosage control for an experiment with live samples. This is an important parameter in studies that require knowing or controlling the effect of ultraviolet radiation on the specimen. In this sense, the development could be extended to control the actual exposure of the sample to UV-light which would be possible with controlled shutters in the light path.

The analysis of light level through each filter showed that the ratio between filters is preserved. This means that any variation in the level of the lamp, considering all wavelengths emitted, will remain proportional after passing the emission filters. However, this requires an additional study to establish the spectral response of the sensor in the range of radiation to adjust the correction for each filter. Future calibrations will be performed for each filter, so that the measurement from the lamp in conjunction with the filter calibration curve will allow calculating more precisely the excitation levels after each filter.

As an additional tool, it is possible to get a dark current image with the exposure time corrected, since the new capture mode makes it a variable for each capture. Therefore, it is possible to have a sample of the noise associated with the image that was captured with exposure control, which is an important parameter when performing quantitative analysis of fluorescence microscope images.

The use of microphone input to acquire the analogue signal of the UV-light monitor was a simple and easy option to connect it to the rest of the equipment because from our software we have control of the CCD device and the motorised stage using some of the available ports. However, the same circuit should be easy to adapt and embed in a micro-controller circuit or any other electronic technology which allows analogue to digital conversion and embeds in the control software of the microscope. At this point, it is convenient to remark on the simplicity of the UV-light monitor, so any microscopy laboratory could rapidly build and test such a device with minimal resources.

Acknowledgments

We thank Enrique Paravani, Silvio Laugero and Javier Adur for their collaboration and support. We want to specially thank Héctor Laforcada for the development of the sound card API for our software, and Michael Thomas Flanagan for his free scientific library for Java. This research was supported by the grant: PID UNER 6082.

References

Adur, J. F. & Schlegel, J. O. (1997) Diseño, desarrollo y construcción de un sistema de avance micrométrico para microscopios fotónicos. Degree thesis, Facultad de Ingeniería. Universidad Nacional de Entre Ríos.

Arndt-Jovin, D. J.; Robert-Nicoud, M.; Kaufman, S. J. & Jovin, T. M. (1985) Fluorescence digital imaging microscopy in cell biology. Science 230(4723), 247-256.

Chen, H.; Swedlow, J. R.; Grote, M.; Sedat, J. W. & Agard, D. (1995) Handbook of biological confocal microscopy. Plenum Press, chapter 13:The collection, processing, and display of digital three-dimensional images of biological specimens, pp. 197-209.

Chen, V. (1995a) Handbook of biological confocal microscopy, Plenum Press, chapter 6: Non-Laser light sources, pp. 99-108.

Diaz-Zamboni, J. E. (2004) Software para usuarios de microscopios de desconvolución digital. Degree thesis, Facultad de Ingeniería, Universidad Nacional de Entre Ríos.

Ferrero, G. J. (1999) Radiómetro ultravioleta eritémico. Degree thesis, Facultad de Ingeniería - Universidad Nacional de Entre Ríos.

Flanagan, M. T. (2010) Java scientific library v6. Department of Electronic Engineering and Department of Computer Science, UCL. http://www.ee.ucl.ac.uk/~mflanaga/java/.

Ghauharali, R. J. & Brakenhoff, G. J. (2000) Fluorescence photobleaching-based image standardization for fluorescence microscopy. J. Microsc. 198(Pt 2), 88-100.

Ghauharali, R. J., Hosftraat, J. W. & Brakenhoff, G. J. (1998) Fluorescence photobleaching-based shading correction for fluorescence microscopy. J. Microsc. 192, 99-113.

Hiraoka, Y., Sedat, J. W. & Agard, D. A. (1987) The use of a charge-coupled device for quantitative optical microscopy of biological structures. Science. 238, 36-41.

Murphy, D. B. (2001) Fundamentals in light microscopy and electronic imaging, Wiley-Liss.

National Semiconductor Corporation (2006) LM555 Timer. Data Sheet.

National Semiconductor Corporation (1995) TL081 Wide Bandwidth JFET Input Operational Amplifier. Data Sheet.

Rasband, W.S. (1997–2010) Image J. US National Institutes of Health, Bethesda, MD, U.S.A. http://rsb.info.nih.gov/ij/.

Sibarita, J.B. (2005) Deconvolution microscopy. Adv. Biochem. Eng. Biotechnol. 95, 201–243.

Song, L., Hennink, E. J., Young, I. T. & Tanke, H. J. (1995) Photobleaching kinetics of fluorescein in quantitative fluorescence microscopy. Biophys. J. 68(6), 2588-2600.

Swedlow, J. R. (2007) Quantitative fluorescence microscopy and image deconvolution. Methods Cell. Biol. 81, 447-465.

Young, I. (1996) Quantitative microscopy. IEEE Eng. Med. Biol. Mag. 15, 59-66.

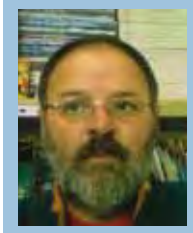
Javier Eduardo Diaz-Zamboni
Microscopy Laboratory, School of Engineering, National University of Entre Ríos, Argentina
javierdiaz@bioingenieria.edu.ar



Javier Eduardo Diaz-Zamboni was born in Paraná, Argentina, in 1978. He received a bioengineering degree from the National University of Entre Ríos, in 2004. He was a pre-degree fellowship researcher at the Microscopy Laboratory at the National University of Entre Ríos, between 2002 and 2004.

He joined the Microscopy Laboratory in 2005. He is currently a research assistant in the Microscopy Laboratory at the School of Engineering, National University of Entre Ríos, and a PhD student at the National University of the Litoral. His research is centred on microscopy image processing and analysis.

Víctor Hugo Casco
Microscopy Laboratory, School of Engineering, National University of Entre Ríos, Argentina
vcasco@bioingenieria.edu.ar



Victor Hugo Casco was born in Los Toldos, Argentina, in 1960. He received a biological sciences degree in 1986 and Doctoral degree in Biology in 1992 from the National University of La Pampa and National University of Cordoba respectively. From 1992 to 2007, Prof. Casco was the Microscopy Laboratory Director.

Between 1996 and 1998, he undertook a postdoctoral fellowship at the University of Ottawa Heart Institute. Since 2007, he has been Full Professor of Cellular and Molecular Biology at the School of Engineering at the National University of Entre Rios. His research interest includes cardiac natriuretic peptides, cell adhesion molecules and modern microscopy technologies.

CONTACTING the RMS

37/38 St Clements, Oxford, OX4 1AJ, UK
Tel. +44 (0) 1865 254760

Administrator
Karen Lonsdale, email: karen@rms.org.uk

For information about meetings and courses
contact: events@rms.org.uk

To join the RMS or for membership enquires
contact: lucy@rms.org.uk

www.rms.org.uk

RMS